GC-MS analysis of aqueous extract of *Nymphaea lotus* and ameliorative potential of its biosynthesized gold nanoparticles against cadmium-induced kidney damage in rats

Victor A. Adebayo [a], Olusola Bolaji Adewale [a,*], Scholastica Onyebuchi Anadozie [a], Olukemi Adetutu Osukoya [a], Tajudeen Olabisi Obafemi [a], Deborah Funmilayo Adewumi [b], Olajumoke Tolulope Idowu [b], Amos Onasanya [a], Abiodun Ayodele Ojo [b]

[a] *Biochemistry Program, Department of Chemical Sciences, Afe Babalola University, Km 8.5, Afe Babalola Way, P.M.B 5454, Ado-Ekiti, 360001, Ado-Ekiti, Nigeria*
[b] *Industrial Chemistry Programme, Department of Chemical Sciences, Afe Babalola University, Km 8.5, Afe Babalola Way, P.M.B 5454, Ado-Ekiti, 360001, Ado-Ekiti, Nigeria*

ARTICLE INFO

ABSTRACT

Plants possess compounds serving as reducing agents for green synthesis of gold nanoparticles (AuNPs), which is currently considered for biomedical application. Exposure to cadmium (Cd) can affect the functional integrity of the several organs such as kidney and liver. *Nymphaea lotus* (NL) is known for its several medicinal properties, including its protective role against tissue damages. This study investigated the bioactive compounds in NL using gas chromatography-mass spectroscopy (GC-MS) and ameliorative potential of its biosynthesized AuNPs (NL-AuNPs) against Cd-induced nephrotoxicity in rats. The presence of bioactive compounds in *N. lotus* was investigated by GC-MS in aqueous extract of NL. Gold nanoparticles were synthesized using aqueous extract of NL. Thirty rats were grouped into six (n = 5). Group 1 served as control, while group 2, 3, 4 and 5 received $CdCl_2$ (10 mg/kg) orally for five days. Thereafter, groups 3, 4, and 5, respectively, received silymarin (75 mg/kg), 5 and 10 mg/kg NL-AuNPs, orally for 14 days, while group 6 received 10 mg/kg NL-AuNPs only. Rats were sacrificed after treatment, and biochemical parameters and kidney histopathology were evaluated. Bioactive compounds of pharmacological importance identified include pyrogallol, oxacyclohexadecan-2-one, 22-Desoxycarpesterol, 7,22-Ergostadienol, β-sitosterol and Dihydro-β-agarofuran. Cadmium caused nephrotoxicity in rats, as evidenced by significant ($p < 0.05$) increase in the levels of kidney function markers (serum urea and creatinine) and inflammatory markers (Interleukin-6 (IL-6) and Nuclear Factor-κB (NF-κB)) when compared with control. These changes were significantly ($p < 0.05$) ameliorated by the spherically-synthesized NL-AuNPs (25–30 nm) with the 5 mg/kg NL-AuNPs more potent against kidney damage induced by Cd in rats but high doses of NL-AuNPs (≥ 10 mg/kg) could be suggested toxic. NL possess phytochemicals capable of reducing gold salts to nanoparticle form, and doses up to 5 mg/kg could be considered safe for the treatment of renal damage occasioned by cadmium.

* Corresponding author. Biochemistry Program, Department of Chemical Sciences, Afe Babalola University, Ado-Ekiti, P.M.B. 5454, Ado-Ekiti 360001, Nigeria.

E-mail addresses: adewaleob@abuad.edu.ng, solaustine2003@yahoo.com (O.B. Adewale).

1. Introduction

Nymphaea lotus, also known as Egyptian white lily, is an aquatic herbaceous plant that belongs to the family of Nymphaeaceae. It grows in Asia and some African countries, and it is used to treat various kinds of ailments in Northern and Western Nigeria [1,2]. It is used locally in the treatment of several diseases such as kidney and bronchial dysfunctions, tumors, bowel complaints, gonorrhea, polyuria and inflammations. It was also reported to possess several medicinal properties including antibacterial, antidiabetic, anti-genotoxic, antioxidant anti-inflammatory and antitumour properties [1–4], and ameliorative potential of its methanolic extract against carbon tetrachloride (CCl_4)-induced hepatoxicity in experimental rats have been reported [5]. The major limitation to the use medicinal plants in the treatment of several ailments include non-specific doses and tissue specificity.

The use of plant and plant products have been preferred in the synthesis of AuNPs due to numerous advantages including readily availability of plants, cost-effectiveness, less or no toxic effects, eco-friendliness, and biocompatibility. These characteristics, among others, have ensured AuNPs as the most widely studied metal nanomaterials for nanomedicine applications. In biological synthesis of AuNPs, many plants and plant products have been involved, acting as capping agaent and in reducing gold salt to its nanoparticle form [6]. These include aqueous extract of *Hibiscus sabdariffa* calyx [7], aqueous extract of *Crassocephalum rubens* leaf [8], leaf extracts of *Annona muricata* [9], and leaf extract of *Dittrichia viscosa* [10]. Several *in vitro* and *in vivo* studies have been reported on the biomedical applications of these plant-synthesized AuNPs [8,10–14]. Their use against various diseases caused by oxidative damage and inflammation, such as cancer, cardiovascular and neurological diseases have been documented [15]. Pharmacological relevance of the plant synthesized AuNPs could be linked to several inherent phytochemicals in plant and the AuNPs to afford specificity to damaged tissues [16].

Cadmium (Cd) toxicity cases have been reported around the world as one of the several health problems that disrupt the normal physiological activities of most organs, leading to death in some cases [17]. It is considered a potential human toxic agent which accumulates in body organs, most especially the kidney and liver (major target organs), and accumulation in the kidney could result in dysfunction of the renal proximal tubule [18,19]. Chronic human exposure from indirect (Cd-contaminated food and industrial waste) and direct (active inhalation of tobacco smoke) sources can exert the generation of reactive oxygen species (ROS) and results in oxidative damage to DNA, lipids, and proteins, and ultimately a decline in the functional integrity of the kidney [19]. Exposure to Cd through agricultural and industrial products, and its unnoticed accumulation over a long period still creates a paucity in health [20, 21]. To afford specificity and high therapeutic load at damaged site, aqueous extract of *N. lotus* was used in the synthesis of AuNPs (NL-AuNPs), and these were used against Cd-induced kidney damage in rats.

2. Materials and methods

2.1. Chemicals and reagents

Gold (III) chloride trihydrate ($HAuCl_4 \cdot 3H_2O$) and cadmium chloride were purchased from Sigma-Aldrich, USA. Renal biomarker (urea and creatinine) kits were obtained from Randox Laboratories Ltd. (Crumlin, Co., Antrim, UK). Silymarin (Silybon) was purchased from Micro Labs Limited (Bengaluru, India. All reagents were of analytical grade.

2.2. Plant material and extraction

N. lotus leaves were obtained and authenticated at the Forestry and Research Institute of Nigeria, Ibadan, where a sample potion was deposited at the Institute's herbarium with a voucher number: FHI 112980. The plant leaves were washed and air-dried for a period of 14 days. The dried leaves were ground into powder using an electric blender. Aqueous extraction was done by boiling the leaf powder in distilled water at 80 °C for 45 min. The resultant mixture was filtered, and was concentrated by drying using water bath at 45 °C.

2.3. Identification of bioactive compounds in aqueous extract of N. lotus using gas chromatography-mass spectroscopy

The GC-MS analysis of aqueous extract of NL leaves was done using the Shimadzu GC-MS-QP2010 SE (Japan), at 250 °C. The split ratio was 10.1, and the carrier gas was nitrogen at an inlet temperature of 250 °C, with a column flow of 3.22 mL/min. The initial column temperature was 60 °C/min, and then increased linearly at 15 °C/min to 120 °C, held for 2 min followed by linear increased temperature 14 °C/min to 300 °C for 4 min. The temperature of the injection port was 250 °C and the GC-MS interface was maintained at 250 °C. The sample was introduced via an all-glass injector working in the split mode, with helium carrier gas rate of 3.22 mL/min. The identification of compounds was accomplished by comparison of retention time, peak area percentage and fragmentation pattern, as well as with mass spectra of the GC-MS. Confirmation of phytochemicals present in *N. lotus* was done by GC-MS with an inbuilt library (NIST11. lib and WILEY).

2.4. Synthesis of AuNPs using aqueous extract of N. lotus leaf

The *N. lotus*-synthesized AuNPs was performed by a method of Geraldes et al. [22], with some modifications. Aqueous leaf extract (100 mg/mL) was added to 1 mM $HAuCl_4 \cdot 3H_2O$ solution in ratio 1:19, respectively, on a magnetic stirrer at 50 °C. The reaction mixture

was stirred continuously and notable changes were recorded at successive period of times until there was a colour change to purple-red. Then, the resultant mixture was centrifuged at 12,000×g for 30 min, and washed twice to remove unconjugated plant extract. The resulting pellet (NL-AuNPs) was air-dried to powdery form for further analyses.

2.4.1. Characterization of N. lotus-synthesized gold nanoparticles

The AuNPs formed were characterized by ultraviolet–visible (UV–Vis) spectroscopy (6715, Jenway) with a range of 300–700 nm to determine the stability and wavelength of the AuNPs, energy-dispersive x-ray spectroscopy (EDX) was performed to investigate the presence of elemental gold, while the transmission electron microscopy (TEM, Fischione's Model 1040 NanoMill) was performed to determine the shape and size of the nanoparticles.

2.5. Experimental animals and grouping

Thirty (30) Wistar rats (*Rattus norvegicus*), aged 10–12 weeks weighing betwwen 160–200 g, were purchased from Veterinary Anatomy animal house, University of Ibadan, Ibadan, and were acclimatized for 14 days at 23 ± 3 °C, with a 12 h light/dark cycle, prior to the start of the experiment. Rats were fed with pelletized food and drinking water throughout the period of the study. Guidelines for Care and Use of Laboratory Animals according to EU Directive 2010/63/EU for animal experiments were adopted in this study, and the animal experiment was approved by the animal research ethics committee of College of Sciences, Afe Babalola University, Ado-Ekiti, Nigeria with ethical number: ABUAD/SCI19/015.

The animals were randomly grouped into six with five rats in each. Group 1 served as control, and received only distilled water throughout the period of the experiment. Cadmium chloride (10 mg/kg, source of cadmium toxicity) was administered intraperitoneally for five days (once daily), to induce kidney toxicity to animals in groups 2, 3, 4, and 5. Animals in group 3 were treated orally with silymarin (75 mg/kg, as standard), while groups 4, 5, and 6 rats were treated orally with 5 mg/kg NL-AuNPs, 10 mg/kg NL-AuNPs, and 10 mg/kg NL-AuNPs only, respectively. All treatments were orally administered to rats daily for 2 weeks after the last dose of the toxicant.

2.5.1. Collection of blood and tissue

Rats were fasted overnight after the last treatment, and were sacrificed via mild exposure to diethyl ether. After loss of sensory, blood was collected via cardiac puncture, was allowed to clot and centrifuged at 3000×g for 10 min to obtain serum. The kidney was quickly removed and washed in ice cold physiological saline to remove blood stains, and were dried using filter paper and weighed. The kidney was homogenized in 0.1 M phosphate buffer at pH 7.4 and centrifuged at 15,000×g for 15 min, and the resulting supernatant was used for subsequent biochemical assays.

2.5.2. Biochemical analysis

Serum levels of urea and creatinine were determined using the protocols of Randox Laboratories test kits (Crumlin, United Kingdom). An index of lipid peroxidation, malondialdehyde (MDA) level in the kidney was estimated according to the method of Varshney and Kale [23] and kidney superoxide dismutase (SOD) level was measured following a protocol by Misra and Fridovich [24], with some modifications. Levels of MDA and SOD in the kidney tissue were expressed as nM/g protein tissue and U/g protein tissue, respectively.

2.5.3. Inflammatory assays

The presence of Interleukin-6 (IL-6) and Nuclear Factor-κB p65 (NF-κB p65) in the kidney was performed using the Sandwich-ELISA principle of IL-6 and NF-κB p65 ELISA kits as described by Engvall and Perlmann [25].

2.5.4. Histology of the kidney

Small pieces of kidney tissues from different groups were cut and fixed in 10% formalin for histopathological analysis. The tissues were dehydrated in graded alcohol and embedded in paraffin. Sections of kidney tissue were mounted on glass slides and were stained with haematoxylin and eosin. Slides were coded and examined under a light microscope by a histopathologist who was ignorant of the treatment groups.

2.6. Statistical analysis

Results were expressed as the mean ± SD (n = 5). Data was analyzed using one-way analysis of variance (ANOVA), and where applicable, intergroup comparison was performed using Tukey's test on GraphPad (Version 5.0). Values were considered statistically significant at $p < 0.05$.

3. Results

3.1. GC-MS analysis of aqueous extract of N. lotus

GC-MS analysis of aqueous extract of *N. lotus* revealed forty-eight compounds (Table 1) with pyrogallol (15.48%) being the most abundance, followed by oxacyclohexadecan-2-one (10.77%), 22-Desoxycarpesterol (8.35%), 7,22-Ergostadienol (5.89%), β-sitosterol

Table 1
Compounds identified in aqueous extract of *Nymphaea lotus* by GC–MS.

Peak No.	Retention time (min)	Compound name	Molecular Formula	Molecular Weight	Area %
1	5.108	2,3-Butanediol	$C_4H_{10}O_2$	90	2.57
2	5.300	*S*-[2-Aminoethyl]-DL-cysteine	$C_5H_{12}N_2O_2S$	164	0.39
3	5.514	2,3-Dihydro-4H-pyran	C_5H_8O	84	0.77
4	5.936	Threitol	$C_4H_{10}O_4$	122	2.12
5	6.070	Erythritol	$C_4H_{10}O_4$	122	2.19
6	6.357	Glycerin	$C_3H_8O_3$	92	1.86
7	6.453	Glycerin	$C_3H_8O_3$	92	3.00
8	6.674	3-(Hydroxymethyl)-2-butanone	$C_5H_{10}O_2$	102	1.27
9	7.197	Dimethylethyleneurea	$C_5H_{10}N_2O$	114	0.85
10	7.653	3,5-Dihydroxy-6-methyl-2,3-dihydro-4H-pyran-4-one	$C_6H_8O_4$	144	0.71
11	7.954	2-[Acetyl (benzoyl)amino]-2-deoxyhexopyranose	$C_{15}H_{19}NO_7$	325	0.34
12	8.293	1,4:3,6-Dianhydro-.alpha.-*d*-glucopyranose	$C_6H_8O_4$	144	0.15
13	8.383	Catechol	$C_6H_6O_2$	110	0.72
14	8.553	Coumaran	C_8H_8O	120	0.18
15	9.793	2-Methoxy-4-vinylphenol	$C_9H_{10}O_2$	150	0.37
16	10.167	Tetrahydroactinidiolide	$C_{11}H_{18}O_2$	182	0.06
17	10.859	Pyrogallol	$C_6H_6O_3$	126	15.48
18	12.866	Pentanoic acid, 5-cyclopropylidene-, ethyl ester	$C_{10}H_{16}O_2$	168	0.17
19	14.367	6-Methyl-cyclodec-5-enol	$C_{11}H_{20}O$	168	0.32
20	14.574	1-Heptadec-1-ynyl-cyclopentanol	$C_{22}H_{40}O$	320	0.18
21	14.652	2,6,8-Trimethylbicyclo [4.2.0]oct-2-ene-1,8-diol	$C_{11}H_{18}O_2$	182	0.51
22	15.260	3,7,11,15-Tetramethyl-2-hexadecen-1-ol	$C_{20}H_{40}O$	296	0.42
23	15.474	*cis*-Z-α-Bisabolene epoxide	$C_{15}H_{24}O$	220	0.14
24	15.581	3,7,11,15-Tetramethyl-2-hexadecen-1-ol	$C_{20}H_{40}O$	296	0.15
25	16.056	Eicosanoic acid	$C_{20}H_{40}O_2$	312	0.55
26	16.261	β-Sitosterol	$C_{29}H_{50}O$	414	1.68
27	16.443	β -Sitosterol	$C_{29}H_{50}O$	414	2.93
28	16.560	β -Sitosterol	$C_{29}H_{50}O$	414	2.00
29	16.804	β -Sitosterol	$C_{29}H_{50}O$	414	3.32
30	16.984	3-Methyl-2-(2-methylene-cyclohexyl)-butan-2-ol	$C_{12}H_{22}O$	182	0.16
31	17.186	5,12-Dihydroxyergost-25 (27)-ene-3,6-dione	$C_{28}H_{44}O_4$	444	0.55
32	18.499	22-Desoxycarpesterol	$C_{37}H_{54}O_3$	546	8.35
33	18.903	7,22-Ergostadienol	$C_{28}H_{46}O$	398	5.89
34	19.136	1,1,6-trimethyl-3-methylene-2-(3,6,9,13-tetramethyl-6- ethenye-10,14-dimethylene-pentadec-4-enyl)cyclohexane	$C_{33}H_{56}$	452	4.60
35	19.233	Viridiflorol	$C_{15}H_{26}O$	222	2.57
36	19.426	*cis*-5,8,11-Eicosatrienoic acid, trimethylsilyl ester	$C_{23}H_{42}O_2Si$	378	1.31
37	19.664	Shyobunone	$C_{15}H_{24}O$	220	1.72
38	19.819	2-Myristynoic acid	$C_{14}H_{24}O_2$	224	1.72
39	19.918	Widdrol	$C_{15}H_{26}O$	222	1.90
40	20.124	*cis*-5,8,11-Eicosatrienoic acid, trimethylsilyl ester	$C_{23}H_{42}O_2Si$	378	0.55
41	20.336	4-(2,2-Dimethyl-6-methylenecyclohexyl)butanal	$C_{13}H_{22}O$	194	0.69
42	20.450	α-Glyceryl linolenate	$C_{21}H_{36}O_4$	352	0.60
43	21.014	15-Chloro-13-oxabicyclo [9.3.1]pentadecane	$C_{14}H_{25}ClO$	244	2.99
44	21.853	Oxacyclohexadecan-2-one	$C_{15}H_{28}O_2$	240	10.77
45	22.037	Patchouli alcohol	$C_{15}H_{26}O$	222	2.23
46	22.233	15-Chloro-13-oxabicyclo [9.3.1]pentadecane	$C_{14}H_{25}ClO$	244	1.73
47	22.434	15-Chloro-13-oxabicyclo [9.3.1]pentadecane	$C_{14}H_{25}ClO$	244	1.55
48	23.094	Dihydro-β-agarofuran	$C_{15}H_{26}O$	222	4.71

(3.32%, 2.93%, 2% and 1.68%) and Dihydro-β-agarofuran (4.71%) among others.

3.2. Biofunctionalization and characterization of AuNPs using N. lotus leaf extract

A colour change to purple-red was observed within 20 min following the addition of the *N. lotus* extract to aqueous HAuCl$_4$ solution (Fig. 1A), indicating the formation of AuNPs (Fig. 1B). The UV–Vis spectroscopy of the synthesized NL-AuNPs reveled an intense peak at 541 nm. The elemental composition of synthesized AuNPs was determined by EDX spectroscopic analysis. The spectrum indicates the presence of gold metal, which constituted the highest percentage of the total composition percentage amidst other elements (Fig. 2A). The size and shape of the synthesized AuNPs were observed by TEM (Fig. 2B). The synthesized AuNPs were mostly spherical, and had a size range of 25–30 nm as observed from the TEM image.
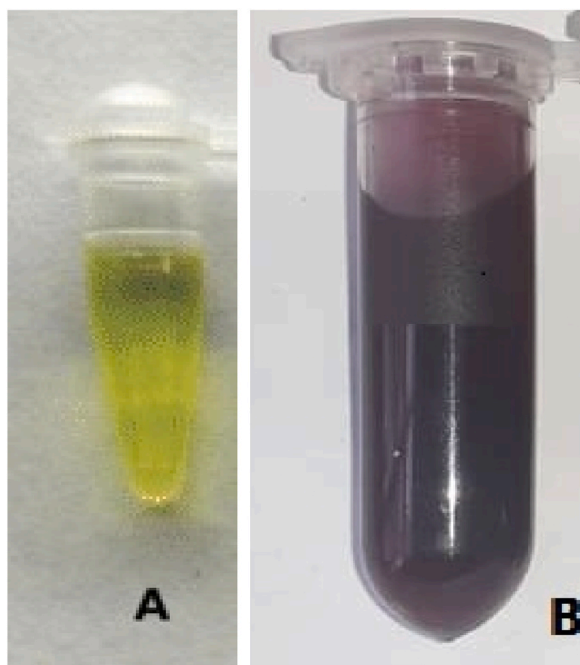
Fig. 1. Observed colour change during the biosynthesis of AuNPs using *Nymphaea lotus*. The $HAuCl_4$ solution before the addition of *N. lotus* (A), the formation of NL-AuNPs after the addition of *N. lotus* to the $HAuCl_4$ solution (B).
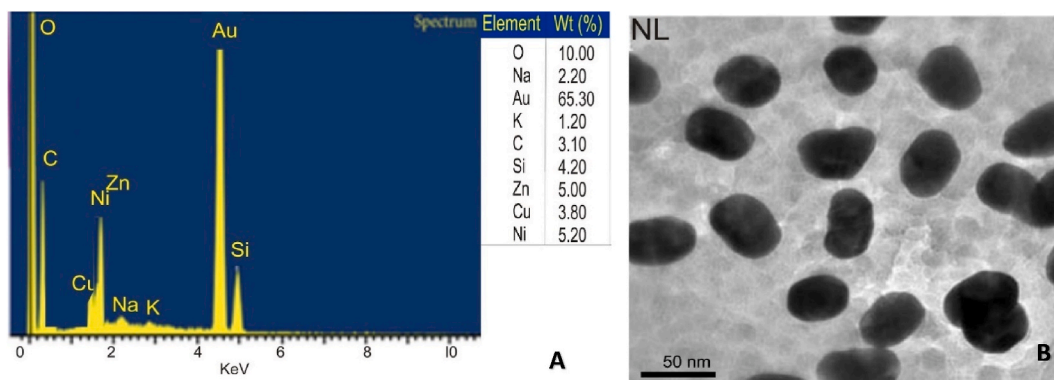

Fig. 2. EDX spectrum showing the elemental composition, with Au having the highest % (A) and transmission electron microscopic images indicating the size and shape (B) of *N. lotus*-synthesized AuNPs. Most of the nanoparticles produced were spherical in shape.

3.3. Effect of kidney function markers

The effect of NL-AuNPs on kidney function markers in rats intoxicated with kidney damage is presented in Fig. 3 (A and B). Exposure of rats to Cd caused a significant increase in the levels of serum urea and creatinine when compared to the control groups. Treatment of Cd administered rats with 5 mg/kg NL-AuNPs caused a significant decrease in the level of serum urea when compared with the untreated Cd intoxicated rat. A significant increase in the level of serum urea was noted when rats treated with 10 mg/kg NL-AuNPs only was compared with the control. Also, a significant ($p < 0.05$) reduction and non-significant reduction in the level of creatinine were noted with 5 and 10 mg/kg, respectively, when compared with the Cd intoxicated rats. A non-significant difference was noted in group treated with 10 mg/kg NL-AuNPs only when compared with the control.

Values are expressed as Mean $\pm$ SD, n = 5. [a]$p < 0.05$ when compared with the control; [b]$p < 0.05$ when compared with the Cd only group; [c]$p < 0.05$ when compared with Cd + 5 mg/kg NL-AuNPs. Cd: cadmium; NL-AuNPs: *N. lotus*-synthesized gold nanoparticles.
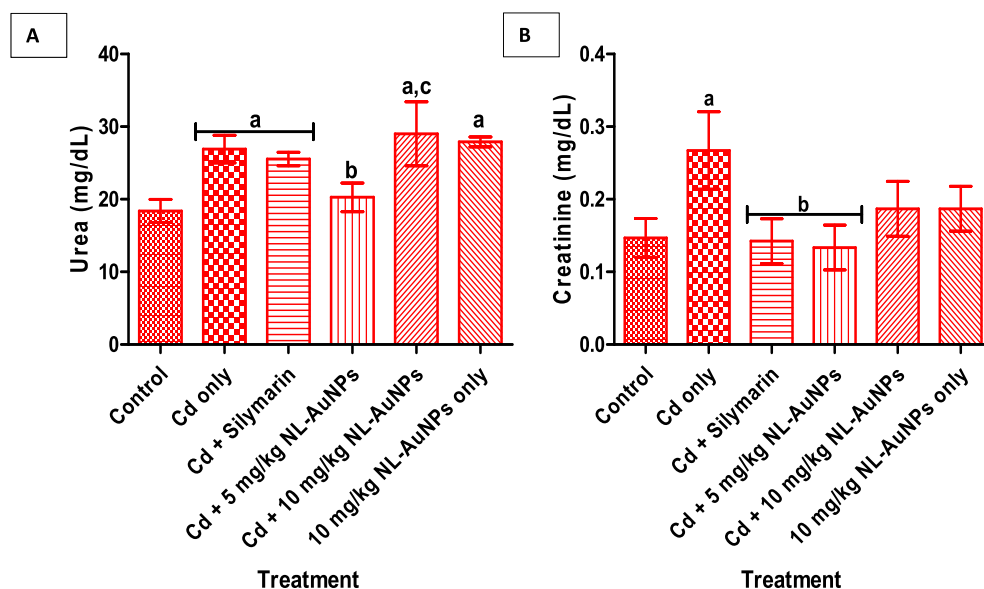
Fig. 3. Effect of *N. lotus*-synthesized AuNPs on the levels of serum urea (A) and creatinine (B) on cadmium-induced kidney damage in rats. NL-AuNPs (mostly at 5 mg/kg) significantly reduced the increased kidney function markers caused by cadmium exposure.

3.4. Effect of NL-AuNPs on kidney malondialdehyde level

The effect of NL-AuNPs on kidney MDA level in Cd-induced kidney damage rats is shown in Fig. 4. A significant increase ($p < 0.05$) in MDA level was noted in rats administered with Cd only when compared with the control group. Treatment of Cd administered rats with 5 mg/kg NL-AuNPs caused a significant decrease ($p < 0.05$) in MDA level when compared with the Cd only treated rats. However, treatment of Cd intoxicated rats with 10 mg/kg NL. AuNPs resulted in non significant difference in MDA level when compared with the untreated Cd intoxicated rats. Rats treated with 10 mg/kg NL-AuNPs only caused a significant increase in MDA level when compared with the control group.

Values are expressed as Mean ± SD, n = 5. [a]$p < 0.05$ when compared with the control group; [b]$p < 0.05$ when compared with the Cd only group; [c]$p < 0.05$ when compared with the Cd + 5 mg/kg NL-AuNPs. Cd: cadmium; NL-AuNPs: *N. lotus*-synthesized gold
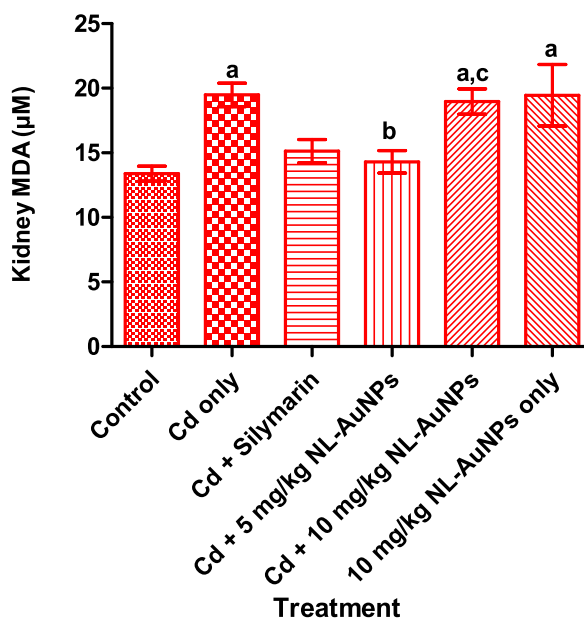

Fig. 4. Effect of NL-AuNPs on the level of kidney malondialdehyde on cadmium-induced renal toxicity in rats. NL-AuNPs (5 mg/kg) significantly reduced the increased kidney MDA caused by cadmium.

nanoparticles.

3.5. Effect of NL-AuNPs on kidney inteleukin-6 level

The presence of IL-6 in the kidney of rats administered with Cd is presented in Fig. 5. The IL-6 level of rats administered with Cd only was significantly ($p < 0.05$) different when compared with the control. Cadmium intoxicated rats treated with silymarin, and both doses of NL-AuNPs resulted in a significant ($p < 0.05$) decrease in the level of IL-6 levels when compared with untreated Cd intoxicated group. A significant ($p < 0.05$) increase in the level of IL-6 was noted in 10 mg/kg NL-AuNPs only when compared with the control group.

Values are expressed as Mean $\pm$ SD, n = 5. [a]$p < 0.05$ when compared with the control group; [b]$p < 0.05$ when compared with the Cd only group. Cd: cadmium; NL-AuNPs: *N. lotus*-synthesized gold nanoparticles.

3.6. Effect of NL-AuNPs on kidney NF-κB level

The presence of NF-κB in the kidney of rats administered with Cd is presented in Fig. 6. Administration of Cd to rats resulted in a significant ($p < 0.05$) increase in the level of NF-κB when compared with the control. However, treatment of the Cd-intoxicated rats with silymarin and 5 mg/kg NL-AuNPs resulted in a significant ($p < 0.05$) decrease in the level of NF-κB when compared with untreated Cd intoxicated rats. A significant difference ($p < 0.05$) was noted in NF-κB level in intoxicated rats treated with the two doses of NL-AuNPs. A non-significant increase was noted in the level of NF-κB in rats treated with only 10 mg/kg NL-AuNPs when compared with the control.

Values are expressed as Mean $\pm$ SD, n = 5. [a]$p < 0.05$ when compared with the control group; [b]$p < 0.05$ when compared with the Cd only group; [c]$p < 0.05$ when compared with the Cd + 5 mg/kg NL-AuNPs. Cd: cadmium; NL-AuNPs: *N. lotus*-synthesized gold nanoparticles.

3.7. Kidney histology

Histology of the kidney is shown in Fig. 7(1–6). Kidney sections of rats in control revealed normal tuft of glomerulus (G), urinary space (black arrow head), distal convoluted tubules (yellow arrow head), proximal convoluted tubules (green arrow head) (Fig. 7(1)). In Cd only group, kidney shows shrunken and degeneration of glomeruli, and urinary space, necrotic and disruption of the renal tubule cells (yellow and green arrow head) (Fig. 7(2)), while rat in Cd + 75 mg/kg silymarin shows a normal tuft of glomerulus (G), urinary space (black arrow head), distal convoluted tubules (yellow arrow head), proximal convoluted tubules (green arrow head) (Fig. 7(3)). Group treated with Cd + 5 mg/kg NL-AuNPs revealed improvement of glomerular tuft, recovery of some renal tubules (Fig. 7(4)), while Cd + 10 mg/kg NL-AuNPs group revealed disrupted renal tubules (Fig. 7(5)), and group treated with 10 mg/kg NL-AuNPs only shows enlarged urinary space and disrupted glomerulus (Fig. 7(6)).

G – glomerulus; black arrow head – urinary space; yellow arrow head – distal convoluted tubules; green arrow head – proximal convoluted tubules.
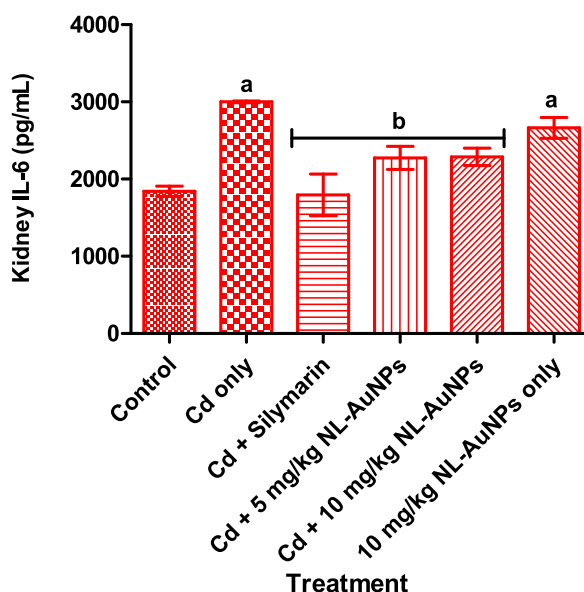

Fig. 5. Effect of NL-AuNP on IL-6 level in kidney tissue of rats administered with cadmium chloride. NL-AuNPs (at both doses tested) significantly reduced the increased presence of IL-6 caused by cadmium exposure.
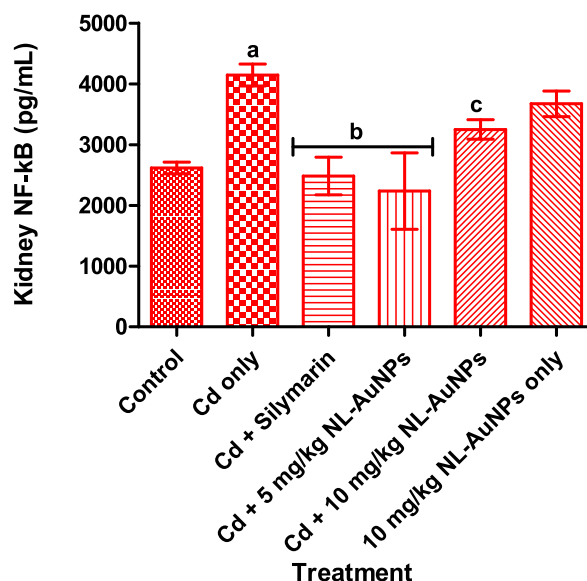
Fig. 6. Effect of NL-AuNP on NF-κB level in kidney tissue of rats administered with cadmium chloride. NL-AuNPs (mostly at 5 mg/kg) significantly reduced the increased presence of kidney NF-κB caused by cadmium exposure.
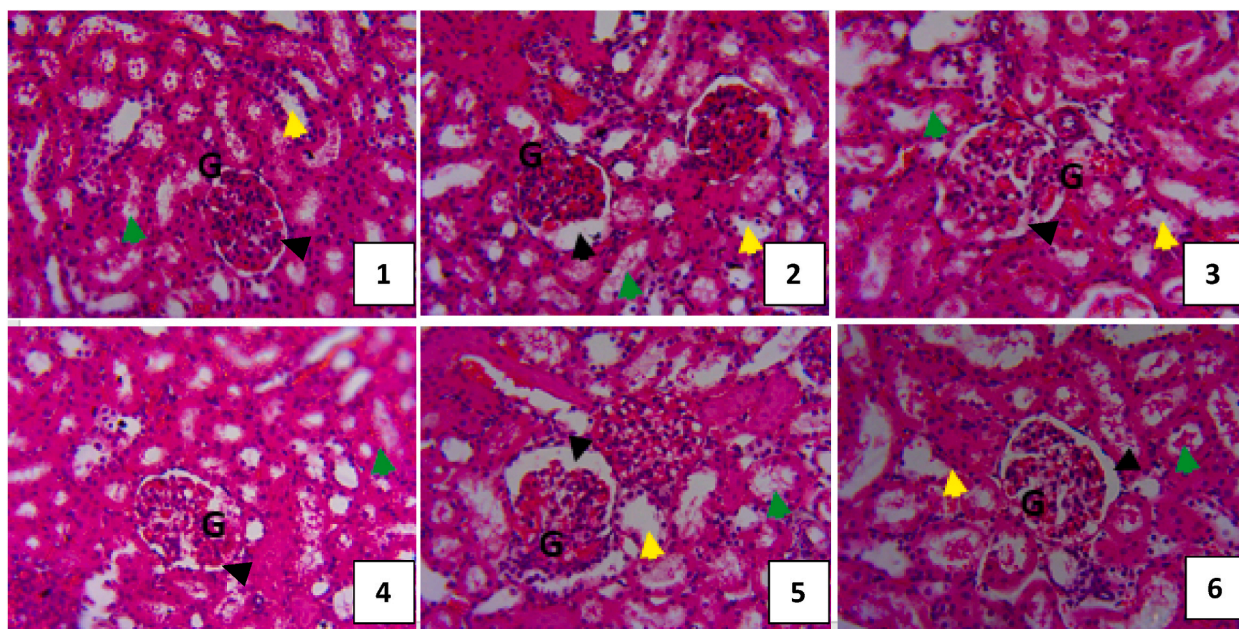

Fig. 7. Photomicrograph of kidney section of rats treated with cadmium for 5 days and NL-AuNPs for 14 days. 1: Control; 2: 10 mg/kg CdCl$_2$ only; 3: 10 mg/kg CdCl$_2$ + 75 mg/kg Silymarin; 4: 10 mg/kg CdCl$_2$ + 5 mg/kg N. *lotus*-AuNPs; 5: 10 mg/kg CdCl$_2$ + 10 mg/kg N. *lotus*-AuNPs; 6: 10 mg/kg N. *lotus*-AuNPs only.

4. Discussion

This study was aimed at investigating the ameliorative potential of NL-synthesized AuNPs on Cd-induced kidney damage in rats. The plant's phytochemical components were evaluated using GC-MS. Kameni et al. [26] qualitatively analyzed the phytochemical components of N. lotus aqueous flower extract and discovered the presence of flavonoids, tannins, saponins, alkaloids, phenolic compounds, glycosides, and cardiac glycosides. In this study, the chromatogram of aqueous extract of NL leaf showed 48 peaks and indicated the presence of nine major compounds, which are of pharmacological importance. For example, the most abundant compound in aqueous extract of NL is pyrogallol, a polyphenol, that has been reported to possess antimicrobial and antioxidant properties,

and it has reportedly been used as a nanocoating in endosseous implant applications [27]. This compound also functions as anti-inflammatory, anti-cancer and anti-proliferative agent [28]. Other compounds, mostly phytosterols (β-sitosterol, 7,22-Ergostadienol and 22-Desoxycarpesterol), are also present in aqueous extract of N. lotus. Phytosterols are sterols present in plants [29], and are known for their pharmacological importance such as their role as antioxidant, anti-atherosclerotic, anti-diabetic, anti-inflammatory, anti-cancer, and cardioprotective agents [30]. β-Sitosterol is a polysterol found richly in nuts, seeds, fruits and vegetables, and various studies have shown that β-sitosterol has anti-diabetic, immunomodulatory, antioxidant, anticancer, anti-inflammatory, and hepatoprotective properties [31,32]. Many of these compounds serve as reducing agents, which could be responsible for the reduction of gold salt to AuNPs, and these compounds could ensure the medicinal importance of N. lotus.

The characteristic colour change that occurred in the reaction between gold solution and aqueous extract of NL is an indication of the synthesis of AuNPs, which may be due to increase in nanoparticle size, reduction reaction and surface plasmon resonance [14]. The AuNPs synthesis was established by UV–Vis spectroscopy with an intense peak at 541 nm, which falls within the range of syntheisized AuNPs [6,11,33,34]. The EDX spectroscopy revealed the presence high % weight of Au (65.30%) with other elements in the following other: $O > Ni > Zn > Si > Cu > C > Na > K$. The presence of elemental oxygen in the EDX spectrum could be as a result of the intermediate molecules necessary for the bonds and stability of the AuNPs synthesized, while the prsence of other elements could be from the plant extract. The size and shape of the NL-AuNPs were revealed by the TEM images. The size and shape (mostly spherical) conforms with those reported previously [35]. The small size of AuNPs (as noted in this study) allows penetration through biological or cellular barriers, thereby enabling enhanced permeability and retention effect on diseased tissues [12,36].

Serum levels of urea and creatinine are generally known as major indicators of kidney functionality, and significant elevation in the levels of these parameters on exposure to Cd has been reported [16,37], indicating injury to the renal tubules [38]. Increased levels of serum urea and creatinine following an exposure of rats to Cd was lowered by NL-AuNPs (5 mg/kg) but not with the 10 mg/kg. This could indicate that the 10 mg/kg NL-AuNPs was not as active as the 5 m/kg NL-AuNPs. In a sub-acute toxicity study, aqueous extract of Nymphaea lotus at high doses (50, 100 and 200 mg/kg) have been reported increased level of creatinine when compared with the control [2], which suggested possible nephrotoxicity. This supports the role of AuNPs in drug delivery to diseased sites.

The MDA (an index of lipid peroxidation) results showed that $CdCl_2$ significantly increased MDA level when compared with the control group, which in line with previous studies [39–41]. However, treatment with NL-AuNPs reversed the peroxidation of lipid in a dose dependent manner as only 5 mg/kg NL-AuNPs showed more potency when compared with the 10 mg/kg dose. The significant difference noted with the administration of 10 mg/kg NL-AuNPs only when compared with the control could indicate the possible nephrotoxic effect of the nanoparticles at higher doses.

Inflammation is an important pathogenic event associated with the toxicity of Cd [42], and increase in IL-6 and NF-κB has been associated with Cd exposure in rats [43–45]. The increased level of IL-6 noted in this study was significantly reduced ($p < 0.05$) by silymarin and both doses of NL-AuNPs. Significant elevation in the level of IL-6 in rats administered with 10 mg/kg NL-AuNPs in comparison with the control is an indication of possible induction of inflammation by high doses of NL-AuNPs. This supports a previous report that dose is an important factor to be considered in the use of AuNPs for biomedical applications [46]. Also, increased presence of NF-κB in the rats' kidney upon in $CdCl_2$ exposure was significantly reversed by silymarin and 5 mg/kg NL-AuNPs but non-significantly with 10 mg/kg NL-AuNPs. This supports the dose-dependent ameliorative potential of NL-AuNPs earlier stated. Reduction in the levels of these inflammatory markers (IL-6 and NF-κB) upon treatment of rats with NL-AuNPs (mostly at 5 mg/kg) supports the anti-inflammatory potential of AuNPs against acute kidney damage [47]. Histopathological analysis of kidney was in line with the various biochemical parameters examined.

5. Conclusions

It can therefore be concluded that major compounds present in *N. lotus* has medicinal properties, and that these compounds have the ability to reduce gold salt to AuNPs. Ameliorative potential against kidney damage occasioned by Cd was in a dose-dependent manner with 5 mg/kg NL-AuNPs more potent. The 10 mg/kg NL-AuNPs could be suggested not potent to reverse Cd-induced nephrotoxicity, and high doses of NL-AuNPs can be suggested toxic to the kidney. Further studies are underway to investigate the toxicity profile of the NL-AuNPs *in vivo*.

Author contribution statement

Victor A. Adebayo: Performed the experiments; Wrote the paper.
Olusola Bolaji Adewale: Conceived and designed the experiments; Analyzed and interpreted the data; Wrote the paper.
Scholastica Onyebuchi Anadozie: Olukemi Adetutu Osukoya: Tajudeen Olabisi Obafemi: Amos Onasanya: Abiodun Ayodele Ojo: Analyzed and interpreted the data; Contributed reagents, materials, analysis tools or data.
Deborah Funmilayo Adewumi: Olajumoke Tolulope Idowu: Contributed reagents, materials, analysis tools or data; Wrote the paper.

Data availability statement

Data will be made available on request.

Declaration of competing interest

The authors declare that they have no known competing financial interests or personal relationships that could have appeared to influence the work reported in this paper.

Acknowledgments

Appendix A. Supplementary data

Supplementary data to this article can be found online at https://doi.org/10.1016/j.heliyon.2023.e17124.

References

[1] A. Wadioni, A.-W. C, A. Ak, W. Vidona, Evaluation of the anxiolytic activity of the leaves of Nymphaea lotus (Water Lily) in mice, Biology & Med. Case Reports 2 (2018).

[2] O. Sharaibi, O. Ogundipe, O. Magbagbeola, M. Kazeem, A. Afolayan, Acute and sub-acute toxicity profile of aqueous leaf extract of Nymphaea lotus linn (nymphaeaceae) in wistar rats, Trop. J. Pharmaceut. Res. 14 (2015) 1231–1238.

[3] B.B. N'guessan, A.D. Asiamah, N.K. Arthur, S. Frimpong-Manso, P. Amoateng, S.K. Amponsah, K.E. Kukuia, J.A. Sarkodie, K.F.-M. Opuni, I.J. Asiedu-Gyekye, R. Appiah-Opong, Ethanolic extract of Nymphaea lotus L. (Nymphaeaceae) leaves exhibits in vitro antioxidant, in vivo anti-inflammatory and cytotoxic activities on Jurkat and MCF-7 cancer cell lines, BMC Complement. Med. Ther. 21 (1) (2021) 22.

[4] I.T. Oyeyemi, O.M. Yekeen, P.O. Odusina, T.M. Ologun, O.M. Ogbaide, O.I. Olaleye, A.A. Bakare, Genotoxicity and antigenotoxicity study of aqueous and hydro-methanol extracts of Spondias mombin L., Nymphaea lotus L. and Luffa cylindrical L. using animal bioassays, Interdiscipl. Toxicol. 8 (4) (2015) 184–192.

[5] I.T. Oyeyemi, O.O. Akanni, O.A. Adaramoye, A.A. Bakare, Methanol extract of Nymphaea lotus ameliorates carbon tetrachloride-induced chronic liver injury in rats via inhibition of oxidative stress, J. Basic Clin. Physiol. Pharmacol. 28 (1) (2017) 43–50.

[6] S.A. Akintelu, B. Yao, A.S. Folorunso, Bioremediation and pharmacological applications of gold nanoparticles synthesized from plant materials, Heliyon 7 (3) (2021), e06591.

[7] S.O. Anadozie, D.O. Effiom, O.B. Adewale, J. Jude, I. Zosela, O.B. Akawa, J.N. Olayinka, S. Roux, Hibiscus sabdariffa Synthesized Gold Nanoparticles Ameliorate Aluminum Chloride Induced Memory Deficits through Inhibition of COX-2/BACE-1 mRNA Expression in Rats, 2023, 104604.

[8] O.B. Adewale, S.O. Anadozie, S.S. Potts-Johnson, J.O. Onwuelu, T.O. Obafemi, O.A. Osukoya, A.O. Fadaka, H. Davids, S. Roux, Investigation of bioactive compounds in Crassocephalum rubens leaf and in vitro anticancer activity of its biosynthesized gold nanoparticles, Biotechnol. Rep. (2020), e00560.

[9] A. Folorunso, S. Akintelu, A.K. Oyebamiji, S. Ajayi, B. Abiola, I. Abdusalam, A. Morakinyo, Biosynthesis, characterization and antimicrobial activity of gold nanoparticles from leaf extracts of Annona muricata, J Nanostructure Chem 9 (2) (2019) 111–117.

[10] S. Ayyoub, B. Al-Trad, A.A.A. Aljabali, W. Alshaer, M. Al Zoubi, S. Omari, D. Fayyad, M.M. Tambuwala, Biosynthesis of gold nanoparticles using leaf extract of Dittrichia viscosa and in vivo assessment of, its anti-diabetic efficacy 12 (12) (2022) 2993–2999.

[11] S.O. Anadozie, O.B. Adewale, M. Meyer, H. Davids, S. Roux, In vitro anti-oxidant and cytotoxic activities of gold nanoparticles synthesized from an aqueous extract of the Xylopia aethiopica fruit, Nanotechnology 32 (31) (2021).

[12] N.R.S. Sibuyi, V.C. Thipe, K. Panjtan-Amiri, M. Meyer, K.V. Katti, Green synthesis of gold nanoparticles using Acai berry and Elderberry extracts and investigation of their effect on prostate and pancreatic cancer cells, Nanobiomedicine 8 (2021), 1849543521995310.

[13] P. Dube, S. Meyer, A. Madiehe, M. Meyer, Antibacterial activity of biogenic silver and gold nanoparticles synthesized from Salvia africana-lutea and Sutherlandia frutescens, Nanotechnology 31 (50) (2020), 505607.

[14] L. Wang, J. Xu, Y. Yan, H. Liu, T. Karunakaran, F. Li, Green synthesis of gold nanoparticles from Scutellaria barbata and its anticancer activity in pancreatic cancer cell (PANC-1), Artif. Cells Nanomed, Biotechnol. 47 (1) (2019) 1617–1627.

[15] W.C. Ko, S.J. Wang, C.Y. Hsiao, C.T. Hung, Y.J. Hsu, D.C. Chang, C.F. Hung, Pharmacological role of functionalized gold nanoparticles in disease applications, Molecules 27 (5) (2022).

[16] O.B. Adewale, S.O. Anadozie, R.T. Okpiri, K.F. Jaiyesimi, O.V. Owolabi, O. Akinlade, T.O. Obafemi, O.A. Osukoya, A. Onasanya, Synthesized gold nanoparticles mediated by Crassocephalum rubens extract down-regulate KIM-1/NGAL genes and inhibit oxidative stress in cadmium-induced kidney damage in rats, Drug Chem. Toxicol. (2022) 1–8.

[17] M.R. Rahimzadeh, M.R. Rahimzadeh, S. Kazemi, A.A. Moghadamnia, Cadmium toxicity and treatment: an update, Caspian J. Intern. Med. 8 (3) (2017) 135–145.

[18] Y. Zhang, Z. Liu, Q. He, F. Wu, Y. Xiao, W. Chen, Y. Jin, D. Yu, Q. Wang, Construction of mode of action for cadmium-induced renal tubular dysfunction based on a toxicity pathway-oriented approach, Front. Genet. 12 (2021).

[19] L.-J. Yan, D.C. Allen, Cadmium-induced kidney injury: oxidative damage as a unifying mechanism, Biomolecules 11 (11) (2021) 1575.

[20] M.M. Rahman, K.F.B. Hossain, S. Banik, M.T. Sikder, M. Akter, S.E.C. Bondad, M.S. Rahaman, T. Hosokawa, T. Saito, M. Kurasaki, Selenium and zinc protections against metal-(loids)-induced toxicity and disease manifestations: a review, Ecotoxicol. Environ. Saf. 168 (2019) 146–163.

[21] Z. Liu, W. Chen, X. He, Evaluation of hyperaccumulation potentials to cadmium (Cd) in six ornamental species (compositae), Int. J. Phytoremediation 20 (14) (2018) 1464–1469.

[22] A.N. Geraldes, A.A. da Silva, J. Leal, G.M. Estrada-Villegas, N. Lincopan, K.V. Katti, A.B. Lugão, Green nanotechnology from plant extracts: synthesis and characterization of gold nanoparticles, Adv. Nano Res. 5 (3) (2016) 176–185.

[23] R. Varshney, R.K. Kale, Effects of calmodulin antagonists on radiation-induced lipid peroxidation in microsomes, Int. J. Radiat. Biol. 58 (5) (1990) 733–743.

[24] H.P. Misra, I. Fridovich, The role of superoxide anion in the autoxidation of epinephrine and a simple assay for superoxide dismutase, J. Biol. Chem. 247 (10) (1972) 3170–3175.

[25] E. Engvall, P. Perlmann, Enzyme-linked immunosorbent assay (ELISA). Quantitative assay of immunoglobulin G, Immunochemistry. 8 (9) (1971) 871–874.

[26] P.M. Kameni, D.P.D. Dzeufiet, D.C. Bilanda, M.F. Mballa, N.Y.S. Mengue, T.H. Tchoupou, A.C. Ouafo, M.C. Ngoungoure, T. Dimo, P. Kamtchouing, Nymphaea lotus linn. (Nymphaeaceae) alleviates sexual disability in L-NAME hypertensive male rats, Evid. Based Complementary Altern. Med. 2019 (2019), 8619283.

[27] N. Kharouf, S. Sauro, L. Hardan, A. Fawzi, I.E. Suhanda, J. Zghal, F. Addiego, C. Affolter-Zbaraszczuk, Y. Arntz, V. Ball, F. Meyer, Y. Haikel, D. Mancino, Impacts of resveratrol and pyrogallol on physicochemical, mechanical and biological properties of epoxy-resin sealers, Bioengineering 9 (3) (2022).

[28] S. Shakya, N. Danshiitsoodol, S. Sugimoto, M. Noda, M. Sugiyama, Anti-Oxidant and anti-inflammatory substance generated newly in paeoniae radix alba extract fermented with plant-derived lactobacillus brevis 174A, Antioxidants 10 (7) (2021).

[29] A. Poli, F. Marangoni, A. Corsini, E. Manzato, W. Marrocco, D. Martini, G. Medea, F. Visioli, Phytosterols, cholesterol control, and cardiovascular disease, Nutrients 13 (8) (2021).

[30] B. Salehi, C. Quispe, J. Sharifi-Rad, N. Cruz-Martins, M. Nigam, A.P. Mishra, D.A. Konovalov, V. Orobinskaya, I.M. Abu-Reidah, W. Zam, F. Sharopov, T. Venneri, R. Capasso, W. Kukula-Koch, A. Wawruszak, W. Koch, Phytosterols: from preclinical evidence to potential clinical applications, Front. Pharmacol. 11 (2021).

[31] S. Jayaraman, N. Devarajan, P. Rajagopal, S. Babu, S.K. Ganesan, V.P. Veeraraghavan, C.P. Palanisamy, B. Cui, V. Periyasamy, K. Chandrasekar, β-Sitosterol circumvents obesity induced inflammation and insulin resistance by down-regulating IKKβ/NF-κB and JNK signaling pathway in adipocytes of type 2 diabetic rats, Molecules 26 (7) (2021).

[32] Y. Yu, Y. Cao, W. Huang, Y. Liu, Y. Lu, J. Zhao, β-Sitosterol ameliorates endometrium receptivity in PCOS-like mice: the mediation of gut microbiota, Front. Nutr. 8 (2021).

[33] C.E.A. Botteon, L.B. Silva, G.V. Ccana-Ccapatinta, T.S. Silva, S.R. Ambrosio, R.C.S. Veneziani, J.K. Bastos, P.D. Marcato, Biosynthesis and characterization of gold nanoparticles using Brazilian red propolis and evaluation of its antimicrobial and anticancer activities, Sci. Rep. 11 (1) (2021) 1974.

[34] M.N. De Canha, V.C. Thipe, K.V. Katti, V. Mandiwana, M.L. Kalombo, S.S. Ray, R. Rikhotso, A. Janse van Vuuren, N. Lall, The activity of gold nanoparticles synthesized using Helichrysum odoratissimum against cutibacterium acnes biofilms, Front. Cell Dev. Biol. 9 (2021).

[35] E.O. Mikhailova, Gold nanoparticles: biosynthesis and potential of biomedical application, J. Funct. Biomater. 12 (4) (2021).

[36] N.R.S. Sibuyi, K.L. Moabelo, A.O. Fadaka, S. Meyer, M.O. Onani, A.M. Madiehe, M. Meyer, Multifunctional gold nanoparticles for improved diagnostic and therapeutic applications: a review, Nanoscale Res. Lett. 16 (1) (2021) 174.

[37] M. Poosa, S.R. Vanapatla, Protective effect of Antigonon leptopus (Hook et. Arn) in cadmium induced hepatotoxicity and nephrotoxicity in rats, Clin. Phytoscience. 6 (1) (2020) 32.

[38] S.M. Dawood, F. Mumtaz, R. Padiya, Zingerone alleviates cadmium-induced nephrotoxicity in rats via its antioxidant and anti-apoptotic properties, Rev. de Cienc. Farm. Basica e Apl. 43 (2022) 1–10.

[39] Z. Song, W. Wang, X. Zhang, H. Yu, C. Qu, S. Dai, X. Wang, Evodiamine attenuates cadmium-induced nephrotoxicity through activation of Nrf2/HO-1 pathway, Trop. J. Pharmaceut. Res. 20 (8) (2022) 1579–1584.

[40] Z. Chen, K. Shi, W. Kuang, L. Huang, Exploration of the optimal strategy for dietary calcium intervention against the toxicity of liver and kidney induced by cadmium in mice: an in vivo diet intervention study, PLoS One 16 (5) (2021), e0250885.

[41] P. Yatmark, N.P. Morales, N. Trakranrungsie, V. Benjacholamas, T. Kampeera, U. Chaisri, Effects of quercetin and vitamin C on pathohistology changes of cadmium-induced organ damage in rat, J. Basic Appl. Pharmacol. 1 (1) (2021) 47–59.

[42] S. Cirmi, A. Maugeri, A. Micali, H.R. Marini, D. Puzzolo, G. Santoro, J. Freni, F. Squadrito, N. Irrera, G. Pallio, M. Navarra, L. Minutoli, Cadmium-induced kidney injury in mice is counteracted by a flavonoid-rich extract of bergamot juice, alone or in association with curcumin and resveratrol, via the enhancement of different defense mechanisms, Biomedicines 9 (12) (2021).

[43] R.S. Almeer, G.I. AlBasher, S. Alarifi, S. Alkahtani, D. Ali, A.E. Abdel Moneim, Royal jelly attenuates cadmium-induced nephrotoxicity in male mice, Sci. Rep. 9 (1) (2019) 5825.

[44] Y.-C. Ou, J.-R. Li, C.-C. Wu, T.-M. Yu, W.-Y. Chen, S.-L. Liao, Y.-H. Kuan, Y.-F. Chen, C.-J. Chen, Cadmium induces the expression of interleukin-6 through heme oxygenase-1 in HK-2 cells and sprague-dawley rats, Food Chem. Toxicol. 161 (2022), 112846.

[45] M.A. Ansari, M. Raish, A. Ahmad, K.M. Alkharfy, S.F. Ahmad, S.M. Attia, A.M.S. Alsaad, S.A. Bakheet, Sinapic acid ameliorate cadmium-induced nephrotoxicity: in vivo possible involvement of oxidative stress, apoptosis, and inflammation via NF-κB downregulation, Environ. Toxicol. Pharmacol. 51 (2017) 100–107.

[46] O.B. Adewale, H. Davids, L. Cairncross, S. Roux, Toxicological behavior of gold nanoparticles on various models: influence of physicochemical properties and other factors, Int. J. Toxicol. 38 (5) (2019) 357–384.

[47] M. Hashim, H. Mujahid, S. Hassan, S. Bukhari, I. Anjum, C. Hano, B.H. Abbasi, S. Anjum, Implication of nanoparticles to combat chronic liver and kidney diseases: progress and perspectives, Biomolecules 12 (10) (2022).